Role of surface defects in colloidal cadmium selenide (CdSe) nanocrystals in the specificity of fluorescence quenching by metal cations

Randa Mrad, Mélanie Poggi, Rafik Ben Chaâbane, Michel Negrerie

Role of surface defects in colloidal cadmium selenide (CdSe) nanocrystals in the specificity of fluorescence quenching by metal cations

Randa Mrad,[a] Mélanie Poggi,[b] Rafik Ben Chaâbane,[a] and Michel Negrerie,*[,c]

[a] *Laboratoire des Interfaces et Matériaux Avancés, Faculté des Sciences de Monastir, Bd. de l'Environnement, 5019 Monastir, Tunisia*.

[b] *Laboratoire de Physique de la Matière Condensée, CNRS UMR7643, Ecole Polytechnique, 91120 Palaiseau, France*.

[c] *Laboratoire d'Optique et Biosciences, INSERM U1182, CNRS UMR7645, Ecole Polytechnique, 91120 Palaiseau, France*.

ABSTRACT

This study aimed to answer the question as whether crystal defects at the surface of soluble capped CdSe nanocrystals (or quantum dots, QDs) in water colloidal suspension are involved in the mechanism of fluorescence quenching induced by metal cations. Nanocrystals of CdSe were synthesized by an aqueous protocol, varying the ratio between the CdSe precursors and the grafted ligand mercaptosuccinic acid (MSA). Changing the MSA/CdSe ratio during synthesis impacts the crystal nucleation growth, which plays an important role in surface construction of CdSe QDs and changes the surface state. In this way, we could modulate the crystal surface defects of CdSe, as verified by analysis of the individual bands which constitute the emission spectra and are associated with different relaxation processes. We found that the various tested metal cations, which interact in solution with the MSA ligand grafted on the QDs, quench their fluorescence differently, depending on the MSA/CdSe ratio used in synthesis. The crystal defects modulate the excitonic relaxation in CdSe and we demonstrated here that the surface defects intervene in the quenching of QDs induced by the binding of cations.

Keywords: Colloidal quantum dots; Surface defects; Excitonic relaxation; Metal cations; Fluorescence quenching

*Corresponding Author

E-mail address: michel.negrerie@polytechnique.fr (M. Negrerie).

1. Introduction

Quantum dots (QDs) have been widely studied for very diverse applications, taking advantage of their size-dependent and tunable optical properties [1,2] which are governed by the nanometric size quantization effect [3]. A large variety of approaches have been established to control the growth of the nanoparticles to the desired size for tuning their photoluminescence, but also to modify their interactions with the medium. The insertion of organic ligands at the semiconductor surface renders the QDs soluble and able to bind particular analytes to these ligands rather than to the semiconductor surface [4]. Such chemical modifications boosted the development of optical sensors for very diverse molecules and ions in solution [5–8], thanks to the change of their photoluminescence induced by the binding of analytes [9]. In most of the cases the sensing is based on the quenching of the emission from the semiconductor QDs [4,9–16]. The surface chemistry of QDs [4,12,13], the nature of the capping ligand, [4,9,10] and the precursors used in the chemistry for grafting ligands [14–16] are determinant for the QDs optical properties. More especially, the emission from the surface bands was shown to depend upon the grafted capping ligands around the QDs [4,9,14,15,17–20]. These ligands have a strong impact on the surface of the QDs, the emission properties [10,14,19,21,22] and may intervene in the fluorescence quenching.

Chen and Rosenzweig [23] published the first example of QDs fluorescence quenching by Cu^{2+} and Zn^{2+} ions interaction with capped CdS nanoparticles in water. Since then, numerous studies have reported the detection of various metal cations by soluble semiconductor QDs (including CdS, CdSe, CdTe, ZnTe) capped with different kinds of organic ligands [23–31] mostly based on the quenching of the QDs fluorescence induced by cations, although some of them reported a fluorescence enhancement [32,33]. Most of these studies were motivated by the toxicity of several metallic ions (such as Cd^{2+}, Hg^{2+}, Pb^{2+}) for health and environment. Cations were hypothesized to bind either directly to the QDs semiconductor surface [32,34,35] or to the grafted ligands surrounding the QDs [27,35]. However, very few studies were endeavored to rationalize the fluorescence quenching induced by cations in water, even though any quantitative analytical method based on fluorescence quenching requires to understand the underlaying mechanisms.

The electron–hole exciton can relaxe through different processes and the quenching mechanism may involve several processes, including non-radiative recombination favored by ions and electron transfer [23,36,37]. Several parameters (nature of semiconductor, size of

QDs, surface defects, nature and density of capping chains) intervene in the photophysical processes and fluorescence. In aqueous solution, metal cations may bind either directly to the semiconductor surface or to the grafted ligand if it possesses a functional group amenable to electrostatic interaction. For example, Cu^{2+} ions in solution with CdSe QDs may induce a cation exchange directly at the QDs surface [38], creating a new recombination channel for exciton relaxation in the resulting Cu^{2+}-doped QDs [20,39], similarly with other dopped chalogenides [40]. However, when metal cations bind to the grafted ligand and induce a quenching [23–31], the relationship between the QD surface state and the emission quenching is barely investigated.

Here, we aimed at understanding whether the crystal defects at the surface of the QDs are involved in the quenching mechanism induced by the binding of a metal cation and the influence of these defects on the specific response between metals. Our approach was to modulate defects by varying the ratio between the precursors of CdSe and the capping ligand MSA in the first step of synthesis, since the Cdse/MSA ratio influences the growth of QDs, as shown previously [15]. The resulting QDs were tested for quenching by numerous metal cations and their fluorescence spectra analyzed in terms of individual emission bands, which appeared greatly altered by the metal cations. This protocol allowed to quantify the contributions of the band edge and the surface emissions [41] due to excitonic relaxation. The crystal defects are favored by the coexistence of both cubic and hexagonal units in CdSe the lattice and a proportion of hexagonal units can be created at the surface of MSA-CdSe QDs [15], acting as "trap" states for excitonic relaxation. Overall, our results show that the surface defects influence the emission spectrum in the absence of cations. Further, we newly demonstrate the role of surface defects in the quenching due to metal cations bound to the QDs and its dependence upon the nature of the metal.

2. Experimental section

2.1. Chemicals

All chemicals were purchased from Sigma-Aldrich and used without further purification. Cadmium acetate dehydrate ($Cd(CH_3COO)_2{\cdot}2H_2O$, 98 %) and selenium dioxide powder (SeO_2, 98 %) were used to provide cadmium and selenium precursors. Sodium borohydride ($NaBH_4$, 98 %) was used as the reducing agent. Mercaptosuccinic acid ($C_4H_6O_4S$, 97 %) was used as the capping ligand. The pH was controled by addition of sodium hydroxide. Distilled water was the solvent for all steps of CdSe QDs synthesis.

The metallic cations to be investigated were released from inorganic soluble salts, purchased either from Sigma-Aldrich Chemicals or from Fluka: NaCl, $CuCl_2$, $HgCl_2$, $CaCl_2$, $CdCl_2$, $CrCl_3$, $CoCl_2$, $FeCl_3$, $MnCl_2$, $MgCl_2$, $NiCl_2$, $Al(NO_3)_2$; $Pb(NO_3)_2$, $Ba(NO_3)_2$, $Zn(C_2H_3O_2)_2$. Stock solutions were prepared at 10^{-3} M in deionized water, the pH was adjusted as needed, and were diluted to the desired concentrations in the QDs solution.

2.2. Synthesis of soluble CdSe nanoparticles in water

We have synthesized, *via* an aqueous method [15,42], four kinds of colloidal MSA-capped CdSe QDs (Scheme S1). These different QDs were obtained by changing the Cd/MSA ratios of the precursors (1/1, 1/1.5, 1/2 and 1/2.5) during the first step of synthesis. Here, the solubilizing ligand MSA is not linked to the QDs post-synthesis but is incorporated during synthesis since the complex Cd–S–R is formed before the QD growth. This complex was first formed by mixing in pure water (under N_2 atmosphere at 24 °C) cadmium acetate dehydrate (50 mL, 6 mM) and MSA (50 mL) whose concentration ranged from 6 to 15 mM, depending upon the desired stoichiometric ratio. The addition of NaOH 1.0 M (10 – 50 µL) allowed to control the pH in order to fully solubilize the Cd^{2+}–MSA precursor formed.

Separately, SeO_2 (10 mL, 3 mM) was mixed with NaOH (5 mL, 1.5 mM) to obtain a water solution of Na_2SeO_3, which was then mixed with the previous solution of Cd^{2+}–MSA. A degased aqueous solution of the reducing agent $NaBH_4$ (5 mL, 7.5 mM) was added at 100 °C under nitrogen atmosphere, until the final solution became yellow, a color characteristic of the solubilized CdSe QDs. The precipitate was finally purified from the unreacted reagents by centrifugation, then washed with methanol three times before drying in a desiccator.

Four different synthesis were performed separately with respective Cd/Se/MSA molar ratios set at 1/0.5/1, 1/0.5/1.5, 1/0.5/2 and 1/0.5/2.5, keeping constant all other parameters, including the Cd/Se ratio. We emphasize that this ratio is not that between the grafted chains and the Cd once the QDs were synthesized, but the ratio between reactants used during the first step of synthesis. The QDs powder was stored at 20 °C in the dark and dissolved in water as needed immediately before use.

2.3. Calculation of the real molar concentration of QDs

We calculated the molecular mass of individual nanoparticles XA-CdSe QDs from their average diameter measured by HRTEM, assuming a spherical shape. From the volume of one CdSe cubic crystal unit (a = b = c = 0.608 nm) we estimated the number of atoms in one QD (for example 668 each of Cd and Se for a 4.2-nm size QD, obtained with the MSA/Cd ratio =

2). We note that a QD with a 3.5 – 4.2 nm diameter possesses a much larger number of crystal units exposed to the surface than within the core. The synthesis process allowed to link the thiol ligand to Cd before the growth of the core crystal lattice and the number of Cd atoms exposed at the surface is larger than in the core. Accordingly, we used the most plausible working hypothesis that one QD comprises ~100 – 150 capping ligands in average. In comparison, the number of ligands is 115 – 225 per QD for CdSe-ZnS QDs capped with polyethylene glycol-aldehyde [43], whose diameter is in the range 3.1 – 4 nm. From the number of atoms in one individual XA-CdSe QD, its molecular mass is directly calculated together with the true molar concentration and the extinction coefficient at the band edge. Our method is based on the direct measurement of the QDs diameter by HRTEM and does not require empirical curve fitting. The mass concentration of colloidal suspension was subsequently adjusted to obtain a QDs molar concentration of 0.1 µM.

2.4. Spectroscopy

Absorption spectra measurements were performed with a Shimadzu UV-1700 spectrophotometer with quartz cuvettes of 1-cm optical path length. The equilibrium fluorescence spectra were measured with a Cary Eclipse spectrometer with the same cuvettes used for absorption. The excitation was set at 350 nm and the slit width was 10 nm for both excitation and emission. A 2-mm thick filter (Schott) blocking wavelengths below 385 nm was placed before the emission entrance slit to stop the scattered excitation light, avoiding the diffracted second order of the excitation at 700 nm. All spectroscopic measurements were performed at 20 °C. The volume of QDs was 2 mL and their concentration was 0.01 – 0.03 $mg \cdot mL^{-1}$. For monitoring the interaction between QDs and cations, a small aliquot of concentrated metallic cation solution (10 µL, negligeable with respect to the volume of QDs) was added into the cuvette to obtain the desired concentration and mixed thoroughly. To allow binding, we waited precisely five minutes before any measurement.

3. Results and discussion

3.1. Fluorescence quenching of MSA-QDs by metal cations

We have previously characterized the physical properties of the synthesized QDs by HRTEM and X-ray diffraction [15]. The diameter of the QDs was statistically determined from electronic microscopy images [15] and increased gradually from 3.5 nm to 5.9 nm as a function of the CdSe/MSA ratio of the reactants during synthesis. The measured parameters

(size, absorption and emission maxima) and calculated ones (molecular weight and extinction coefficient) are summarized in Table 1. Firstly, changing the molar ratios (Cd/MSA = 1/1, 1/1.5, 1/2 and 1/2.5) impacts the size of the MSA-capped CdSe QDs [thereafter refered to as CdSe(1), CdSe(1.5), CdSe(2) and CdSe(2.5)].

Table 1. Properties of the synthesized MSA-CdSe QDs.

QDs refered to as	MSA/Cd ratio	D_{TEM} (*a*) (nm)	MW_{QD} (*b*) ($g \cdot mol^{-1}$)	ε (*c*) ($M^{-1} \cdot cm^{-1}$)	λ_{edge} (nm)	λ_{em} (nm)	E_g (eV)
CdSe(1)	$R_1 = 1.0$	3.5 ± 0.1	0.90×10^5	1.0×10^5	420	503, 615 (*d*)	2.50
CdSe(1.5)	$R_2 = 1.5$	4.0 ± 0.1	1.27×10^5	8.0×10^5	430	550	2.40
CdSe(2)	$R_3 = 2.0$	4.2 ± 0.1	1.47×10^5	15×10^5	439	554	2.25
CdSe(2.5)	$R_4 = 2.5$	5.9 ± 0.2	3.75×10^5	14×10^5	508	580	2.02

(*a*) Determined from high resolution transmission electronic microscopy.
(*b*) Molecular weight calculated from the size.
(*c*) Absorption coefficient at λ_{edge} (maximum of first excitonic band).
(*d*) Respectively, excitonic core emission and surface emission.

The absorption maxima of the first excitonic band (Fig. S1) and the fluorescence emission (Fig. 1) were both shifted to longer wavelengths (Table 1), according to the confinement effect linked to increased size (gaining energy with the increased difference between the conduction and the valence bands as the size decreases) [3,18,41]. The excitonic emission band is identified by considering that its energy position depends on the CdSe QDs size and has a higher energy than the surface defect emission band. The fluorescence spectrum of the smallest QD discloses an excitonic emission band (Fig. 1A) at higher energy (503 nm) which is sharper and clearly distinct from the defect trap emission at 615 nm. This separation of both bands is pronounced for smaller QDs [41,44]. Well separated components appear when using a low concentration of ligand during synthesis because the proportion of surface defects increases with the density of grafted chains. Then, progressive quenching of the excitonic emission is induced by increased concentration of MSA.

Importantly, the crystal defects at the surface of the semiconductor core, to which trap-state emission is associated, depends on the reacting ratio CdSe/MSA as shown by the variations of the emission profile. Trap-state emission can also be modulated by other means, for example by varying the refluxing time during synthesis (creating sulfur vacancies in CdS) [45]. Besides defects, the capping ligands can also influence the emissive trap sites, as observed by Baker and Kamat after the exchange of dodecylamine for MPA [44], inducing a drastic decrease of the band edge emission and increase of the trap state emission.

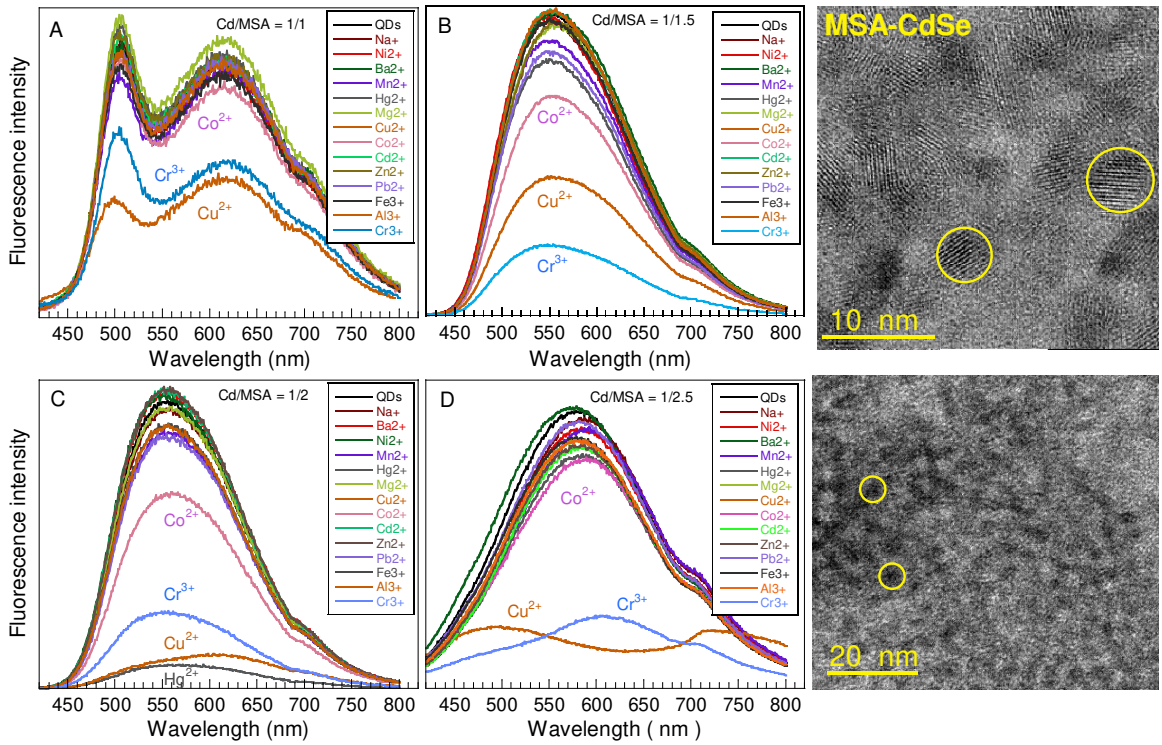

Fig. 1. Fluorescence spectra of CdSe nanocrystals with different precursor Cd/MSA ratios before and after the addition of different metal cations at 10 µM in water. The concentration of QDs is 0.1 µM. Reacting ratios are : 1/1 (**A**); 1/1.5 (**B**); 1/2 (**C**) and 1/2.5 (**D**). Excitation at λ_{ex} = 350 nm; pH = 7.8; T = 20 °C. Examples of high resolution transmission electronic microscopy images for the CdSe(2.5) QDs. The diameters of MSA-CdSe QDs determined from HRTEM images are: 3.5 nm for CdSe(1), 4.0 nm for CdSe(1.5), 4.2 nm for CdSe(2) and 5.9 nm for CdSe(2.5).

We evaluated the influence of the Cd/MSA ratio on the quenching efficiency of the QDs emission by cations. Indeed, the carboxylate groups of MSA are susceptible of binding cations and we tested a large variety of metal ions in water (Na^+, Pb^{2+}, Ni^{2+}, Mn^{2+}, Co^{2+}, Hg^{2+}, Zn^{2+}, Ba^{2+}, Cd^{2+}, Cu^{2+}, Fe^{3+}, Al^{3+}, Cr^{3+} and Fe^{3+}, all at 10 µM). These cations induced different changes of intensity but the fluorescence emission of all MSA-CdSe nanocrystals was substantially quenched in the presence of Cu^{2+} and Cr^{3+} ions at 10 µM (Fig. 1). In addition, CdSe(1.5) and CdSe(2) QDs were more sensitive to Co^{2+} (Fig. 1B and C), whereas CdSe(2) QDs were strongly sensitive to Hg^{2+} (Fig. 1C) contrarily to other QDs. The sensitivity toward Cu^{2+} and Cr^{3+} ions is inverted between CdSe(1.5) and CdSe(2) QDs (Fig. 1B,C) and the fluorescence spectrum of CdSe(2.5) QDs in the presence of both cations discloses very different spectral band shapes (Fig. 1D).

For all QDs, the fluorescence intensity decreased as a function of increasing concentration of particular cations (Fig. 2), however the spectral profiles evolved differently, depending on the nature of both QDs and cations. The quenching of CdSe(1) due to Cu^{2+} is accompanied by a small shift of the band centered at 615 nm (Fig. 2A) whereas Cu^{2+} at 20 µM produced a

large spectral red-shift for CdSe(1.5), (2) and (2.5) (Fig. 2B,C,G). The spectral evolution is similar for CdSe(1.5) and CdSe(2), but the latter is more sensitive to Cu^{2+}, whereas Cr^{3+} did not induce a spectral shift for CdSe(1.5) and CdSe(2) (Fig. 2E,F). The concentration increase of both Cu^{2+} and Cr^{3+} had a dramatic effect on the spectral shape of CdSe(2.5) (Fig. 2G,H) with a considerable shift of the main emission band as its intensity decreased.

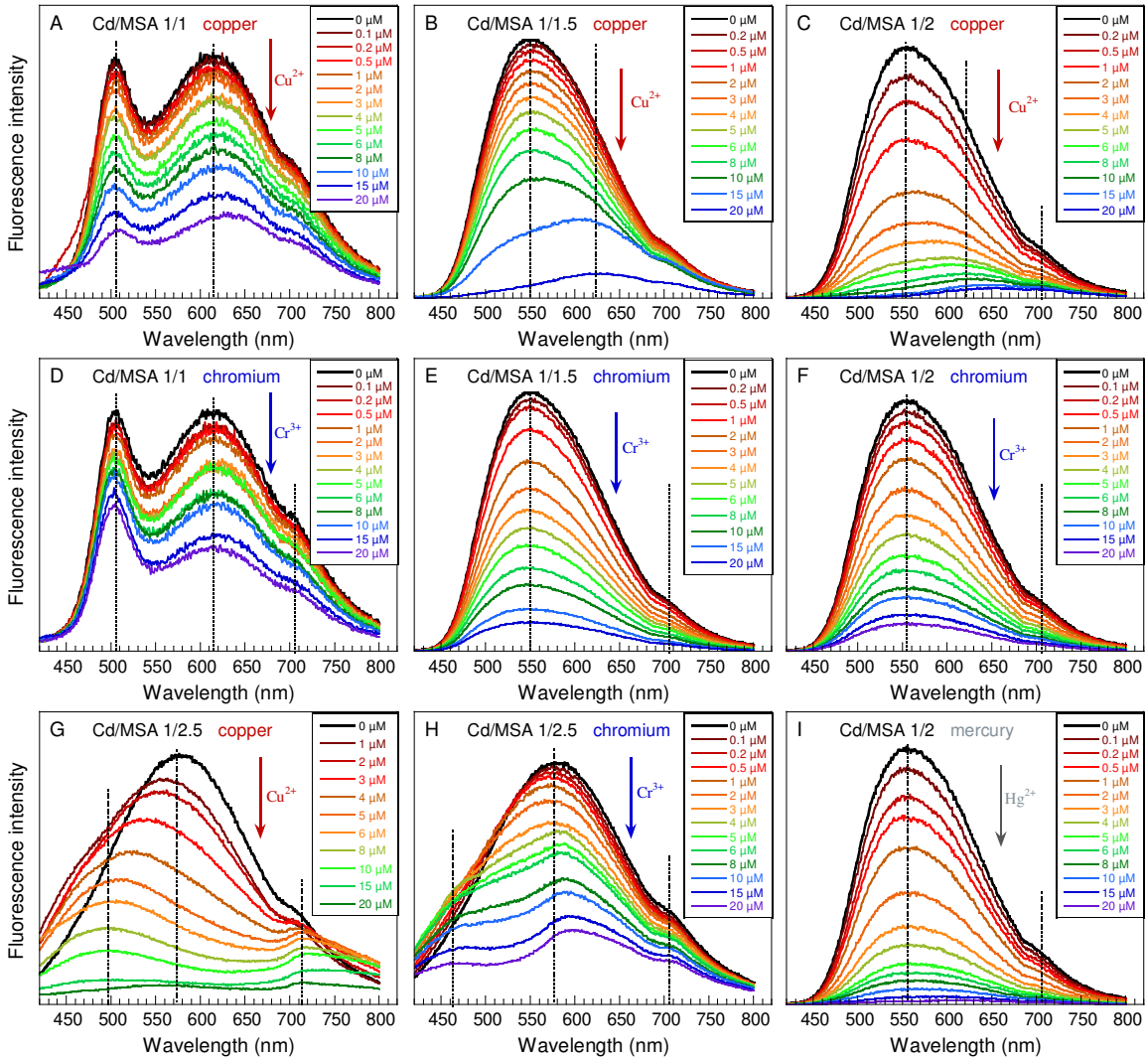

Fig. 2. Effect of Cu^{2+} (A, B, C, G), Cr^{3+} (D, E, F, H) and Hg^{2+} (I) concentration on the fluorescence of MSA-CdSe QDs in water with different precursor Cd/MSA ratios as indicated in the panels. λ_{ex} = 350 nm. The concentration of QDs is 0.1 µM. The molar ratio between QDs and cations varies accordingly between 1 and 200.

The fluorescence quenching induced by Hg^{2+} occurred only for CdSe(2) QDs (Fig. 2I) without noticeable spectral shift. The same spectral evolution was observed for the binding of Hg^{2+} to MSA-Au QDs [46], whose emission was also quenched by Cu^{2+} and Pb^{2+}, but not Co^{2+} and Cr^{3+}, implying that the nature of the metal cation is crucial in the quenching mechanism for semiconductor QDs. The red shift of the emission in the presence of Cu^{2+} (Fig.

2B,C) was also observed for CdS QDs in propanol [34] when Cu^{2+} binds to the CdS surface. Co^{2+} ions also quenched the QDs fluorescence, essentially for CdSe(1.5) and CdSe(2) QDs (Fig. 3) but in a less pronounced manner than other cations, with still half emission intensity at 20 µM with respect to the QDs alone.

Since it is known that semiconductor QDs properties may evolve over time, we have verified whether the quenching induced by cations occurred in the same manner for QDs newly synthesized and for QDs stored for six months in the dark at 20 °C. An example is given in Fig. S2 for CdSe(2) QDs interacting with Cu^{2+} and Cr^{3+}. This storage did not alter the quenching of the QDs emission, a behavior fully compatible with the fact that some cations induce quenching whereas other cations do not.

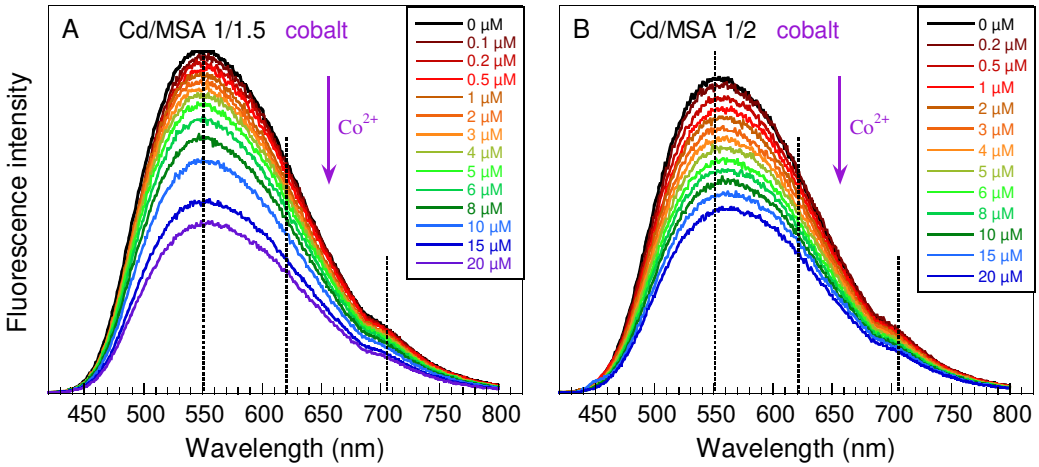

Fig. 3. Effect of increasing Co^{2+} concentration on the fluorescence of CdSe QDs with the precursor Cd/MSA ratios of 1/1.5 (**A**) and 1/2 (**B**). Excitation wavelength: 350 nm. pH = 7.8; T = 20 °C. The concentration of QDs is 0.1 µM.

The change of spectral profile simultaneously with the emission quenching by cations is not systematic, but was reported in many cases, pointing out the multiplicity of reactions. Various quenching responses to cations (Ag^{+}, Co^{2+}, Cu^{2+}, Pb^{2+}, Fe^{3+} and Hg^{2+}) were also observed for diverse QDs capped with different thiolate ligands, [26,45,47–50] as we observe here, suggesting a general mechanism. The emission quenching is also induced by several metals for other thiol-capped QDs, such as MPA-CdS (Co^{2+}, Ni^{2+}) [45], Cys-CdTe (Cu^{2+}, Ag^{+}, Hg^{2+}) [49], Cys-CdS (Cu^{2+}, Co^{2+}, Ni^{2+}, Hg^{2+}) [50] and hydroxybenzyl-Cys-CdS (Cu^{2+}, Co^{2+}, Hg^{2+}) [51]. In these studies, a red shift dependent on the metal concentration was also observed for Cu^{2+} and in a lesser extent for Hg^{2+}, highlighting the relation between the nature of the cations and the spectral profile, that is, the relative contributions of the core and surface emissions. A detailed analysis requires to distinguish the individual spectral components.

3.2. Identification of the emission spectral components

In order to identify the emission relaxation processes we analyzed the fluorescence spectra by fitting them to a sum of Gaussian components. In the absence of metal cations (Fig. 4A-D), the spectra comprise three emission bands, whose relative intensity depends (given in Table S1) on the Cd/MSA ratio. To assign the excitonic band edge emission, we considered that its energy position depends on the CdSe QDs size effect, [3, 18, 52–53] which correlates with the position of the excitonic absorption band (Fig. S1). Accordingly, the Gaussian component 1, of higher energy, was assigned to the core emission (direct exciton recombination) because its central wavelength position follows the QDs size increase (Table 1). This assignment agrees well with spectra which also disclose well separated components [41,45].

There does not necessarily exist a formal relationship for the ratio of intensities of first and second components (0.79, 0.52, 0.64 and 0.71, respectively for the four QDs, Fig. 4A-D). This could possibly occur in a regime where the Cd/MSA ratio has a "linear" influence on QDs growth, which seems to be the case for CdSe(1.5), (2) and (2.5), yielding a trend of increasing ratio (0.52, 0.64 and 0.71). However, the Cd/MSA 1:1 ratio was intentionally chosen as extreme case in order to act more drastically on the crystal defects, and the ratio of intensities of first and second components has no reason to follow a particular trend. This is why the emission spectrum of CdSe(1) QDs (Fig. 4A) has a different shape than others.

The emission bands 2 and 3, of lower energy, therefore involve recombination due to defects in the crystal units at the surface of QDs (trap states) [54–56]. These defects can be favored by the coexistence of both cubic and hexagonal units in the CdSe lattice, modulated by the Cd/MSA ratio [15]. The proportion of recombination from core exciton and from defect trap states is very sensitive [3,52,57] and the observed change of spectral profiles in the absence of metal cations reflects the changes of surface states of the QDs [34,47]. Depending upon the interacting cations, the individual emission bands evolved differently regarding their positions and relative amplitudes and are now compared in the presence of 10 μM cations (Fig. 4).

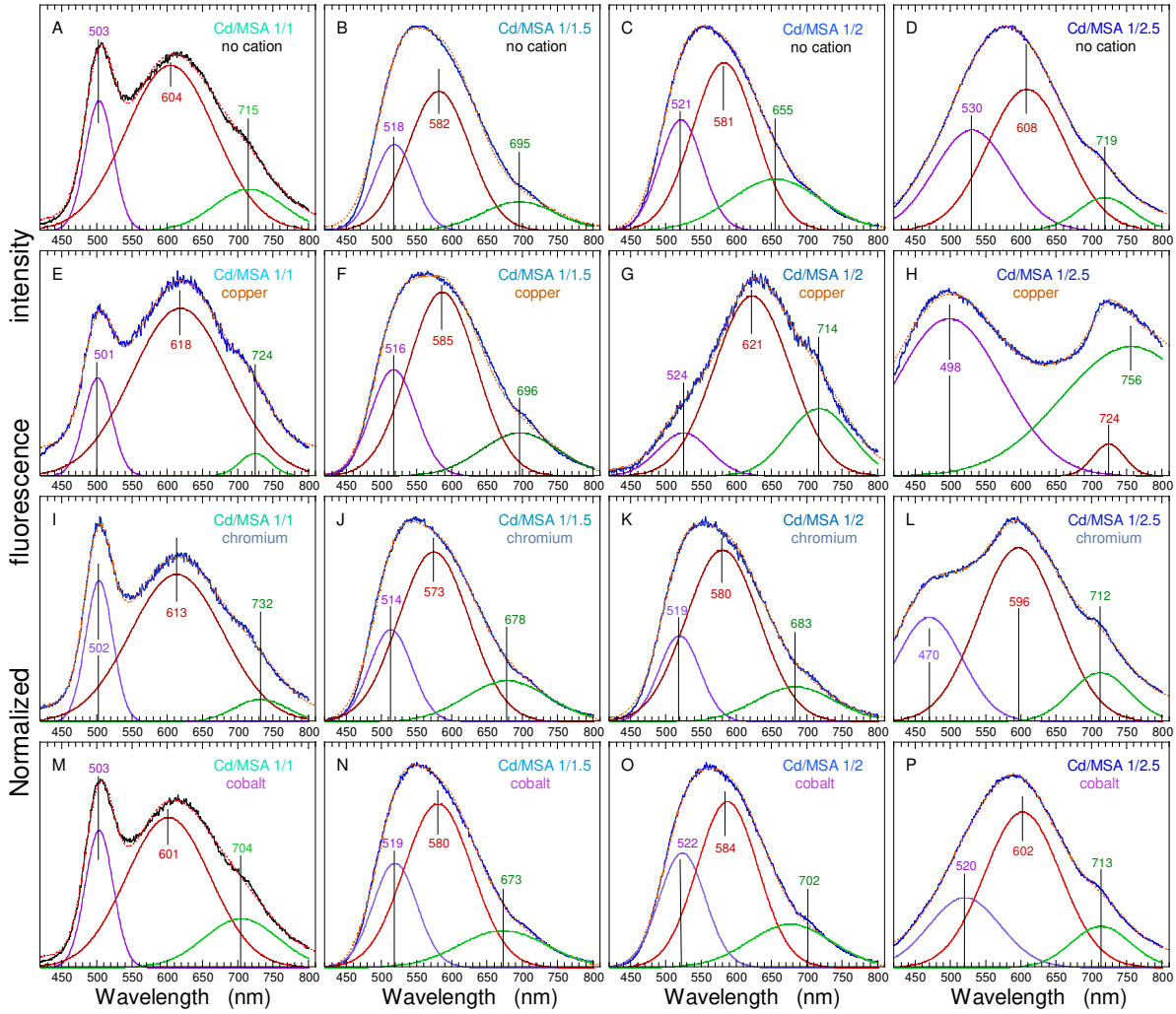

Fig. 4. Spectral analysis of the fluorescence emission of the various MSA-CdSe QDs in the absence (A-D) or presence of 10 µM metal ions: Cu^{2+} (E-H), Cr^{3+} (I-L), Co^{2+} (M-P). All spectra were fitted to a sum of three individual Gaussian functions. The orange dotted line superposed to the raw spectra is the result of the fit. See Table S1 for the fitting parameters. Since the spectra are normalized, the relative intensity of the bands can be compared. CdMSA(2)–Hg^{2+} is shown in Fig. S3.

3.3. Comparing cations for a particular QD (vertical dimension of Fig. 4)

For CdSe(1), the three cations (Cu^{2+}, Cr^{3+} and Co^{2+} at 10 µM) did not induce a shift of the core exciton emission, within the error of the fit (502 ± 1 nm) whereas Cu^{2+} and Cr^{3+} induced a red shift (+14 and +9 nm) of the surface emission (Table S1). Cu^{2+} induced an increase of the relative intensity of surface emission (618 nm). Similarly, for CdSe(1.5) the position of the core exciton emission is not changed (516 ± 2 nm), but its surface emission is altered differently, with a shift induced by Cr^{3+} (–9 nm) in opposite way compared with CdSe(1). For CdSe(2) the three cations did not induce a significant shift of the core exciton emission (521 ± 2 nm), but Cu^{2+} induced a large red shift (+40 nm) of the surface emission (Fig. 4G), contrarily to Cr^{3+} for which the position is unchanged (Fig. 4K). Co^{2+} changed neither the position of emission bands nor their relative intensities.

Remarkably, only CdSe(2) was quenched by Hg^{2+}, which induced a red shift of all emission bands (+6 nm for exciton core emission; +15 nm for surface emission) and an increase of the relative intensity of surface emission (Fig. S3). This observation agrees with reports showing that incorporation of Hg^{2+} into the lattice lowers the band gap energy of CdTe and CdSe QDs [58] and induces a decrease of the quantum yield [59]. We note that Hg is the largest atom among metals inducing a fluorescence quenching of our QDs (Pb^{2+} produced a very small reaction). Beside electrostatic interaction with carboxylates, the binding to the CdSe surface critically depends on its accessibility which appears optimized for the interaction with Hg^{2+} when using the ratio Cd/MSA = 2. The interpretation of quenching by surface binding of Hg^{2+} agrees with dynamic quenching (Fig. 5 and 6) which critically depends on molecular encounters.

For CdSe(2.5), which is the most affected by surface defects, both Cu^{2+} and Cr^{3+} induced a blue shift of the core emission (Fig. 4H and L), indicating their direct binding to the semiconductor, whereas Cu^{2+} drastically affected the surface emission band. Co^{2+} induced a small blue shift of both the core (−10 nm) and surface (− 6 nm) emissions.

3.4. Comparing QDs for a particular cation (horizontal dimension of Fig. 4)

Differences between cations are also evident. The quenching by Cu^{2+} resulted in the most important effects, but opposite for CdSe(2) and CdSe(2.5), leading to a red shift of surface emission with high relative intensity for the former, but to a blue shift of the core emission with larger relative intensity for the latter. Cr^{3+} induced band shift only for CdSe(2.5) (Fig. 4L), albeit able to quench all four QDs. Co^{2+} is the quencher which less perturbes the spectral profile, suggesting a single mode of binding.

Thus, the four metals Cu^{2+}, Cr^{3+}, Co^{2+} and Hg^{2+} act differently regarding the surface defects. The characteristics of the defects (density, nature, accessibility) depend upon the QDs synthesis [4,9,14,15,17–20] and greatly affect their photophysics [4,9,19,22]. The binding of a particular cation may occur both to the surface of the semiconductor lattice or to the carboxylate groups of MSA, and the proportion of both types of binding should depend on the cation and on the surface defects. The surface emission is more affected than the core emission for three QDs. Only in the extreme case of CdSe(2.5) the core (band edge exciton) emission is altered, which could be indicative of a charge transfer process [41]. However, the quenching due to the binding of cations to the charged carboxylate groups is conveyed by the link between the ligand and the surface defects and cannot be explained by charge transfer [41].

3.5. Quenching is both static and dynamic

Although the cation-QD mixture was allowed to equilibrate before recording the emission spectra, the static character of the quenching is not obligatory. The Stern-Volmer representation of the fluorescence quenching (Fig. 5) suggests the occurrence of both static and dynamic quenching processes. For CdSe(2)-Cu^{2+} and CdSe(2)-Hg^{2+}, and in a less pronounced manner for CdSe(2.5)-Cu^{2+} and CdSe(1.5)-Cr^{3+}, the curves were fitted to a quadratic relation. In the other cases [CdSe(1)-Cu^{2+}, CdSe(1.5)-Cu^{2+}, CdSe(1)-Cr^{3+}, CdSe(2.5)-Cr^{3+}, CdSe(1.5)-Co^{2+}, CdSe(2)-Co^{2+}] a linear equation was sufficient to fit data.

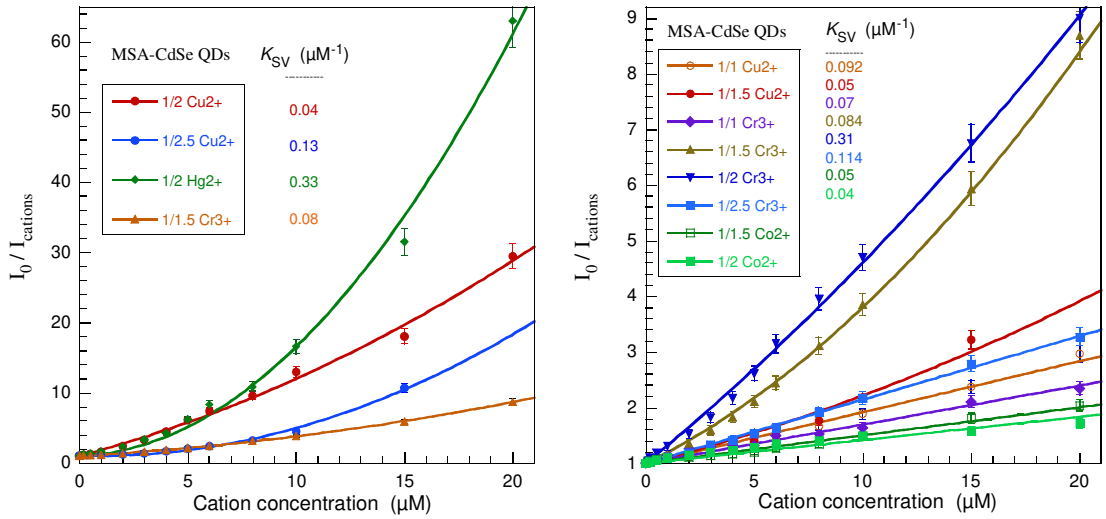

Fig. 5. Stern-Volmer representation of the MSA-CdSe QDs fluorescence quenching by cations. The data (from Figs. 2 and 3) were fitted using either a linear or a second-order Stern-Volmer equation. The upward curved relation indicates mixed static and dynamic processes. The corresponding K_{SV} constants are indicated for each fitted curves. CdSe(1.5)-Cr^{3+} is present in both panels.

The fluorescence lifetime for CdSe(2) interacting with Cu^{2+}, Cr^{3+} and Hg^{2+} (Fig. 6) decreases as a function of cations concentration in the three cases, pointing out a dynamic process. For these cations, the quadratic dependence of the intensity ratio I_0/I (Fig. 5) indicates the simultaneous presence of both static and dynamic quenching. Fundamentally, the static quenching occurs through a pre-established equilibrium of bound cations to the carboxylate groups of the ligands, resulting from a property of the QD-cation system as a whole, not from encounters of excited QDs with cations in solution. The simultaneous presence of a dynamic component is not surprising, since cations have the ability to diffuse to the semiconductor surface.

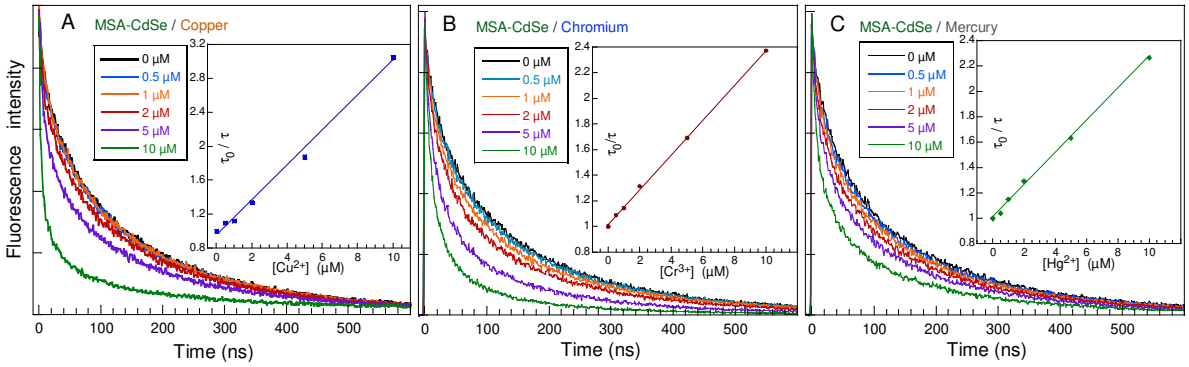

Fig. 6. Fluorescence decays of MSA-CdSe QDs (reacting ratio Cd/MSA = 1/2) as a function of cations concentration: Cu^{2+} (A), Cr^{3+} (B) and Hg^{2+} (C). Inserts: evolution of the ratio τ_0/τ as a function of cations concentration. Excitation wavelength: 372 nm. Emission wavelength: 550 nm. Optical pathlength = 1 cm. pH = 7.8; T = 20 °C. The concentration of QDs is 0.1 µM.

To verify the effect of the number of carboxylate groups in one ligand, we have synthesized CdSe QDs (with the same synthesis ratio CdSe/ligand = 1/2) using thioglycolic acid (TGA) and mercaptosuccinic acid (MPA) as the ligands, which both possess only one carboxylate group, contrary to MSA which has two groups (Fig. S4). The fluorescence of MPA-CdSe(2) is quenched by Cu^{2+}, Cr^{3+} and Co^{2+}, as is MSA-CdSe, whereas that of TGA-CdSe(2) is quenched mainly by Cr^{3+} at 10 µM (Fig. 7). In addition, TGA has also an effect on the relative intensity between band edge and surface emissions. Thus, the position of the TGA carboxylate, closer to the QD surface compared to MPA, may influence its incorporation during synthesis and the surface state of TGA-CdSe. Remarkably, both TGA- and MPA-capped QDs appeared twice less sensitive than MSA-CdSe QDs as a function of cation concentration (Fig. 2C and F). Since MSA possesses two carboxylates and can bind two cations per grafted ligand, this observation emphasizes the role of these charged groups.

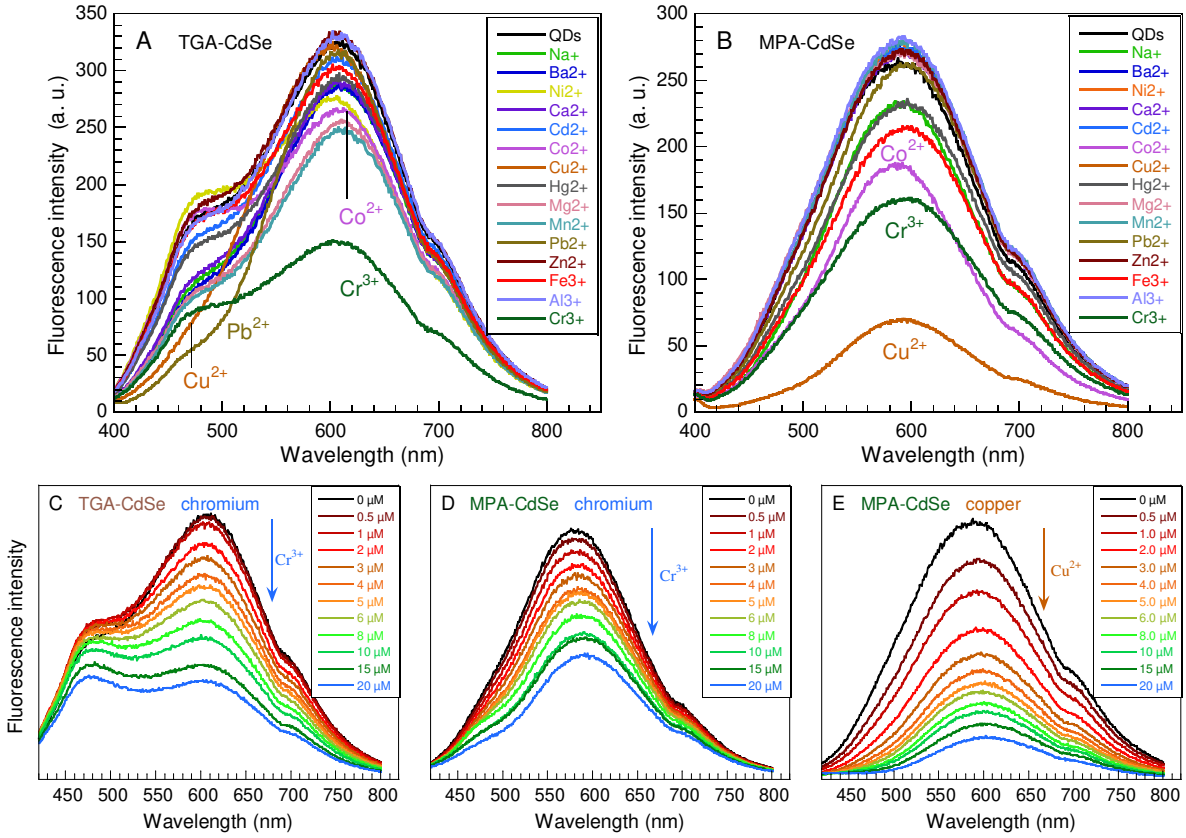

Fig. 7. Fluorescence spectra of CdSe nanocrystals functionalized with thioglycolic acid (A) and mercaptosuccinic acid (B) as capping ligands, both with reacting ratio Cd/ligand = 1/2, before and after the addition of different metal cations at 10 µM in water. Comparison of the fluorescence quenching due to increasing concentration of Cr^{3+} on TGA-CdSe (C) and on MPA-CdSe (C), and of Cu^{2+} on MPA-CdSe (E) QDs in water. pH = 7.8. λ_{ex} = 350 nm. The concentration of QDs is 0.1 µM.

In some studies [60] the reabsorption of the QDs emission by cations (sometimes called "inner filter") was proposed as a quenching mechanism. We readily discarded this hypothesis by measuring the absorption spectra of all cations (Fig. S5). The spectrum of Cr^{3+} discloses an absorption band centered at 576 nm with a very low molar extinction coefficient (ε = 10 $M^{-1}{\cdot}cm^{-1}$) whereas Cu^{2+} and Co^{2+} have a broad band centered at ~800 nm and ~520 nm with coefficients ε = 20 and 32 $M^{-1}{\cdot}cm^{-1}$ respectively. Albeit Cr^{3+} and Co^{2+} absorption spectra overlap the emission of all QDs, they cannot absorb efficiently the QD emission. Therefore, a Förster energy transfer or "inner filter" due to cations must be discarded as the general photophysical quenching mechanism.

4. Conclusions and perspectives

Here, we have synthesized QDs whose surface defects were modulated by varying the ratio of precursors (Cd/thiol) during synthesis [15]. As a consequence, the individual emission

bands associated with surface defects changed. Furthermore, in the presence of metal cations bound to the carboxylates of MSA, the induced quenching was also altered. Overall, these results demonstrate the essential role of the surface state in the quenching of fluorescence induced by metal cations. In this case, the energy level of surface defects (either Cd^{2+} or Se^{2-} vacancies; Fig. 8) are changed by both the grafted ligands and cations, changing the probability of exciton recombination through non radiative pathways.

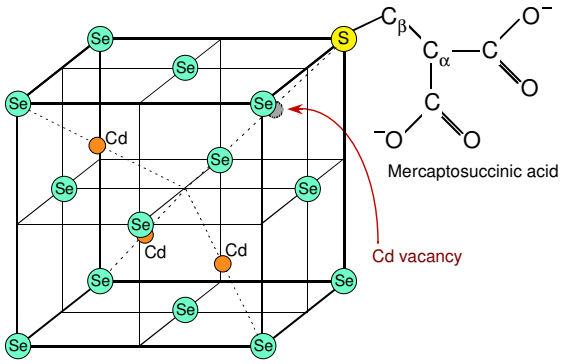

Fig. 8. Representation of a crystal unit at the surface of a CdSe nanocrystal with a Cd vacancy adjacent to the sulfur atom of mercaptosuccinic acid. This scheme was inspired from Ref. [61]. The mercaptosuccinic acid chain is not exactly scaled with the crystal unit to emphasize the Cd vacancy.

The importance of the exciton to ligand vibrational coupling in functionalized QDs is established [17,61,62], based on energy transfer [62,63], and appears fundamental for determining their photophysical properties. Our result fully agrees with the concept that the QD-ligands vibronic coupling is influenced by surface defects. Considering this coupling, we have recently demonstrated that the binding of cations (which are heavy atoms) modifies the vibrational Raman modes of the grafted ligand [64], consequently the hypothesis emerges as the role played by the exciton-vibrational coupling in the QD emission. This coupling, modulated by surface defects, can be involved in the quenching by cations and we will verify this hypothesis by probing the evolution of ligands vibrational spectrum using time-resolved Raman spectroscopy in the picosecond time-range [65], relevant for exciton relaxation [63]. The latter occurs through energy transfer from electronic levels to phonon modes associated with the QD surface [66] or to ligands vibrational modes [66,67]. Future works should vibrationally probe, not only the interaction of colloidal QDs with metal cations, but also with various kinds of analytes including biological relevant ones [68].

So far, many studies have addressed QDs as sensors for metal cations based on fluorescence quenching. However, numerous reported cases disclose a large variability in sensitivity and specificity (even for similar QDs) and it appears that the quenching induced by cations highly depends on the QDs synthesis. We emphasize that, whereas soluble QDs provide a powerful tool for detecting particular analytes in water, the design of any QD-based sensor requires a deep understand the underlying mechanism and an very precise control of QDs synthesis. The exciton to ligand vibrational coupling is a quite new concept in the study of QDs. Understanding its fundamentals will foster the development of QDs-based sensors, bringing keys to their design when interacting in a biological environment [68], and can be extended to thin film materials.

Declaration of interest

The authors declare no competing financial interest.

Acknowledgements

R. M. acknowledges a travel research fellowship "Bourse d'Alternance" from the Tunisian Government. We thank the CIMEX team (*Centre Interdisciplinaire de Microscopie Electronique en transmission de l'Ecole Polytechnique*) for the help provided in acquiring TEM data. R. M. thanks Nassim Ben Brahim (*Laboratoire des Interfaces et Matériaux Avancés, Faculté des Sciences de Monastir, Tunisia*) for help in data analysis.

References

[1] A.P. Alivisatos, Semiconductor clusters, nanocrystals and quantum dots, Science 271 (1996) 933–938.

[2] Z. Cao, Z. Gu, J.L. Zeng, J.H. Liu, Q. Deng, J.B. Fan, J.N. Xiang, A novel fluorescent probe for copper ions based on polymer-modified CdSe/CdS core/shell quantum dots. Anal. Sci. 27 (2011) 643–647.

[3] J. Jasieniak, L. Smith, J. van Embden, P. Mulvaney, Re-examination of the size-dependent absorption properties of CdSe quantum dots. J. Phys. Chem. C 113 (2009) 19468–19474.

[4] M.A. Boles, D. Ling, T. Hyeon, D.V. Talapin, The surface science of nanocrystals. Nat. Mater. 15 (2016) 141–153.

[5] H. Mattoussi, J.M. Mauro, E.R. Goldman, G.P. Anderson, V.C. Sundar, F.V. Mikulec, M.G. Bawendi, Self-assembly of CdSe-ZnS quantum dot bioconjugates using an engineered recombinant protein. J. Am. Chem. Soc. 122 (2000) 12142–12150.

[6] J.M. Costa-Fernandez, R. Pereiro, A. Sanz-Medel, The use of luminescent quantum dots for optical sensing. Trends Anal. Chem. 25 (2006) 207–218.

[7] X.H. Bu, Y.M. Zhou, M. He, Z.J. Chen, T. Zhang, Bioinspired, direct synthesis of aqueous CdSe quantum dots for high-sensitive copper(II) ion detection. Dalton Trans. 42 (2013) 15411–15420.

[8] Z. Chen, D. Wu, Monodisperse BSA-conjugated zinc oxide nanoparticles based fluorescence sensors for Cu^{2+} ions. Sens. Actuators B Chem. 192 (2014) 83–91.

[9] M.M. Krause, P. Kambhampati, Linking surface chemistry to optical properties of semiconductor nanocrystals. Phys. Chem. Chem. Phys. 17 (2015) 18882–18894.

[10] M.M. Krause, J. Mooney, P. Kambhampati, Chemical and thermodynamic control of the surface of semiconductor nanocrystals for designer white light emitter. ACS Nano 7 (2013) 5922−5929.

[11] P. Kambhampati, Hot exciton relaxation dynamics in semiconductor quantum dots: radiationless transitions on the nanoscale. J. Phys. Chem. C 115 (2011) 22089–22109.

[12] S.K. Han, C. Gu, M. Gong, S.H. Yu, A Trialkylphosphine-driven chemical transformation route to Ag- and Bi-based chalcogenides. J. Am. Chem. Soc. 137 (2015) 5390−5396.

[13] C. Gu, S.J. Hu, X.S. Zheng, M.R. Gao, Y.R. Zheng, L. Shi, Q. Gao, X. Zheng, W.S. Chu, H.B. Yao, J. Zhu, S.H. Yu, Synthesis of sub-2 nm iron-doped $NiSe_2$ nanowires and their surface-confined oxidation for oxygen evolution catalysis. Angew. Chem. Int. Ed. 57 (2018) 4020−4024.

[14] V. A. Amin, K. O. Aruda, B. Lau, A. M. Rasmussen, K. Edme, E. A. Weiss, Dependence of the band gap of CdSe quantum dots on the surface coverage and binding mode of an exciton-delocalizing ligand, methylthiophenolate. J. Phys. Chem. C 119 (2015) 19423–19429.

[15] R. Mrad, M. Poggi, N. Ben Brahim, R. Ben Chaâbane, M. Negrerie, Tailoring the photophysical properties and excitonic radiative decay of soluble CdSe quantum dots by controling the ratio of capping thiol ligand. Materialia 5 (2019) 100191.

[16] S.K. Han, C. Gu, S. Zhao, S. Xu, M. Gong, Z. Li, S.H. Yu, Precursor triggering synthesis of self-coupled sulfide polymorphs with enhanced photoelectrochemical properties. J. Am. Chem. Soc. 138 (2016) 12913−12919.

[17] T.G. Mack, L. Jethi, M. Andrews, P. Kambhampati, Direct observation of vibronic coupling between excitonic states of CdSe nanocrystals and their passivating ligands. J. Phys. Chem. C 123 (2019) 5084–5091.

[18] L. Jethi, T.G. Mack, M.M. Kraus, S. Drake, P. Kambhampati, The effect of exciton-delocalizing thiols on intrinsic dual emitting semiconductor nanocrystals. Chem. Phys. Chem. 17 (2016) 665–699.

[19] M.M. Krause, L. Jethi, T.G. Mack, P. Kambhampati, Ligand surface chemistry dictates light emission from nanocrystals. J. Phys. Chem. Letters 6 (2015) 4292–4296.

[20] R. Viswanatha, S. Brovelli, A. Pandey, S.A. Crooker, V.I. Klimov, Copper-doped inverted core/shell nanocrystals with “permanent” optically active holes. Nano Letters 11 (2011) 4753−4758.

[21] Kambhampati, P. On the kinetics and thermodynamics of excitons at the surface of semiconductor nanocrystals: are there surface excitons? Chem. Phys. 446 (2015) 92–107.

[22] H.H.Y. Wei, C.M. Evans, B.D. Swartz, A.J. Neukirch, J. Young, O.V. Prezhdo, T.D. Krauss, Colloidal semiconductor quantum dots with tunable surface composition. Nano Lett. 12 (2012) 4465−4471.

[23] Y. Chen, Z. Rosenzweig, Luminescent CdS quantum dots as selective ion probes. Anal. Chem. 74 (2002) 5132–5138.

[24] R. Kho, C.L. Torres-Marteiz, R.K. Mehra, A simple colloidal synthesis for gram-quantity production of water-soluble ZnS nanocrystal powders. J. Colloid Interface Sci. 227 (2000) 561–566.

[25] Y.B. Lou, Y.X. Zhao, J.X. Chen, J.J. Zhu, Metal ions optical sensing by semiconductor quantum dots. J. Mater. Chem. C 2 (2014) 595–613.

[26] A.H. Gore, D.B. Gunjal, M.R. Kokate, V. Sudarsan, P.V. Anbhule, S.R. Patil, G.B. Kolekar, Highly selective and sensitive recognition of cobalt(II) ions directly in aqueous solution using carboxyl-functionalized CdS QDs as a naked eye colorimetric probe: applications to environmental analysis. ACS Appl. Mater. Interfaces 4 (2012) 5217–5226.

[27] K.M. Gatt´as-Asfura, R.M. Leblanc, Peptide coated CdS quantum dots for the optical detection of copper(II) and silver(II). Chem. Comm. 21 (2003) 2684–2685.

[28] X. Michalet, F.F. Pinaud, L.A. Bentolila, J.M. Tsay, S. Doose, J.J. Li, G. Sundaresan, A.M. Wu, S.S. Gambhir, S. Weiss, Quantum dots for live cells, in vivo imaging, and diagnostics. Science 307 (2005) 538–544.

[29] M. Kanimoto, T. Shiragami, C. Pac, S. Yanagida, Semiconductor photocatalysis Effective photoreduction of carbon dioxide catalyzed by ZnS quantum crystallites with low density of surface defects. J. Phys. Chem. 96 (1992) 3521–3526.

[30] N. Ben Brahim, M. Poggi, J.-C. Lambry, N. Bel Haj Mohamed, R. Ben Chaâbane, M. Negrerie, Density of grafted chains in thioglycerol-capped CdS quantum dots determines their interaction with aluminium(III) in water. Inorg. Chem. 57 (2018) 4979–4988.

[31] N. Bel Haj Mohamed, N. Ben Brahim, R. Mrad, M. Haouari, R. Ben Chaâbane, M. Negrerie, Use of MPA-capped CdS quantum dots for sensitive detection and quantification of Co^{2+} ions in aqueous solution. Anal. Chim. Acta 1028 (2018) 50–58.

[32] D.E. Moore, K. Pate, Q-CdS photoluminescence activation on Zn^{2+} and Cd^{2+} salt introduction, Langmuir 17 (2001) 2541–2544.

[33] J.L. Chen, C.Q. Zhu, Functionalized cadmium sulfide quantum dots as fluorescence probe for silver ion determination. Anal. Chim. Acta 546 (2005) 147–153.

[34] A.V. Isarov, J. Chrysochoos, Optical and photochemical properties of nonstoichiometric cadmium sulfide nanoparticles, surface modification with copper(II) ions. Langmuir 13 (1997) 3142–3149.

[35] N. Ben Brahim, N. Bel-Haj Mohamed, M. Echabaane, M. Haouari, R. Ben Chaâbane, M. Negrerie, H. Ben Ouada, Thioglycerol-functionalized CdSe quantum dots detecting cadmium ions. Sens. Actuators B - Chemical 220 (2015) 1346–1353.

[36] J.R. Lakowicz, Principles of Fluorescence Spectroscopy. 3rd edition (2006) ISBN 978-1-4757-3061-6 Plenum Press, New York.

[37] M.T. Fernández-Argüelles, W.J. Jin, J.M. Costa-Fernández, R. Pereiro, A. Sanz-Medel, Surface-modified CdSe quantum dots for the sensitive and selective determination of Cu(II) in aqueous solutions by luminescent measurements. Anal. Chim. Acta 549 (2005) 20–25.

[38] H. Li, R. Brescia, R. Krahne, G. Bertoni, M.J.P. Alcocer, C. D'Andrea, F. Scotognella, F. Tassone, M. Zanella, M. De Giorgi, L. Mann, Blue-UV-emitting ZnSe(dot)/ZnS(rod) core/shell nanocrystals prepared from CdSe/CdS nanocrystals by sequential cation exchange. ACS Nano 6 (2012) 1637−1644.

[39] R.W. Meulenberg, T. van Buuren, K.M. Hanif, T.M. Willey, G.F. Strouse, L.J. Terminello, Structure and composition of Cu-doped CdSe nanocrystals using soft X-ray absorption spectroscopy. Nano Letters 4 (2004) 2277−2285.

[40] C. Pu, H. Qin, Y. Gao, J. Zhou, P. Wang, X. Peng, Synthetic control of exciton behavior in colloidal quantum dots. J. Am. Chem. Soc. 139 (2017) 3302–3311.

[41] M.M. Krause, T.G. Mack, L. Jethi, A. Moniodis, J.D. Mooney, P. Kambhampati, Unraveling photoluminescence quenching pathways in semiconductor nanocrystals. Chem. Phys. Letters 633 (2015) 65–69.

[42] N. Ben Brahim, N. Bel-Haj Mohamed, M. Poggi, R. Ben Chaâbane, M. Haouari, H. Ben Ouada, M. Negrerie, Interaction of L-cysteine functionalized CdSe quantum dots with metallic cations and selective binding of cobalt in water probed by fluorescence. Sens. Actuators B - Chemical 243 (2017) 489–499.

[43] N. Zhan, G. Palui, J.-P. Merkl, H. Mattoussi, Bio-orthogonal coupling as a means of quantifying the ligand density on hydrophilic quantum dots. J. Am. Chem. Soc. 138 (2016) 3190−3201.

[44] D.R. Baker, P.V. Kamat, Tuning the emission of CdSe quantum dots by controlled trap enhancement. Langmuir 26 (2010) 11272−11276.

[45] N. Mahapatra, S. Panja, A. Mandal, M. Halder A single source-precursor route for the one-pot synthesis of highly luminescent CdS quantum dots as ultra-sensitive and selective photoluminescence sensor for Co^{2+} and Ni^{2+} ions. J. Mater. Chem. C 2 (2014) 7373−7384.

[46] X. Xiong, X. Lai, J. Liu, Mercaptosuccinic acid-coated NIR-emitting gold nanoparticles for the sensitive and selective detection of Hg2+. Spectrochim. Acta Part A 188 (2018) 483–487.

[47] C. Dong, H. Qian, N. Fang, J. Ren, Study of fluorescence quenching and dialysis process of CdTe quantum dots, using ensemble techniques and fluorescence correlation spectroscopy. J. Phys. Chem. B 110 (2006) 11069–11075.

[48] T. Zeng, Y. Hu, N. Wang, C. Xia, S. Li, Y. Zu, L. Liu, Z. Yao, Y. Zhao, H.-C. Wu, Effects of different metal ions on the fluorescence of CdSe/ZnS quantum dots capped with various thiolate ligands. Phys. Chem. Chem. Phys. 15 (2013) 18710−18715.

[49] J. Chen, A.F. Zheng, Y. Gao, C. He, G. Wu, Y. Chen, X. Kai, C. Zhu, Functionalized CdS quantum dots-based luminescence probe for detection of heavy and transition metal ions in aqueous solution. Spectrochim. Acta Part A 69 (2008) 1044−1052.

[50] T. Gong, J.F. Liu, X. Liu, J. Liu, J. Xiang, Y. Wu, A sensitive and selective sensing platform based on CdTe QDs in the presence of L-cysteine for detection of silver, mercury and copper ions in water and various drinks. Food Chem. 213 (2016) 306−312.

[51] S. Akshya, P.S. Hariharan, V.V. Kumar, S.P. Anthony, Surface functionalized fluorescent CdS QDs: Selective fluorescence switching and quenching by Cu^{2+} and Hg^{2+} at wide pH range. Spectrochim. Acta Part A 135 (2015) 335−341.

[52] M. Tamborra, M. Striccoli, R. Comparelli, M.L. Curri, A. Petrella, A. Agostiano, Optical properties of hybrid composites based on highly luminescent CdS nanocrystals in polymer. Nanotechnol. 15 (2004) 240–244.

[53] Y.H. Zhang, H.S. Zhang, M. Ma, X.F. Guo, H. Wang, The influence of ligands on the preparation and optical properties of water-soluble CdTe quantum dots. Appl. Surf. Sci. 255 (2009) 4747–4753.

[54] A.D. Dukes, M.A. Schreuder, J.A Sammons,. J.R. McBride, N.J. Smith, S.J. Rosenthal, Pinned emission from ultrasmall cadmium selenide nanocrystals. J. Chem. Phys. 129 (2008) 121102.

[55] H. Sharma, S.N. Sharma, G. Singh, S.M. Shivaprasad, Effect of ratios of Cd, Se in CdSe nanoparticles on optical edge shifts and photoluminescence properties. Physica E 31 (2006) 180−186.

[56] A.R. Kortan, R. Hull, R.L. Opila, M.G. Bawendi, M.L. Steigerwald, P.J. Carroll, L.E. Brus, Nucleation and growth of CdSe on ZnS quantum crystallite seeds and vice versa, in inverse micelle media. J. Am. Chem. Soc. 112 (1990) 1327–1332.

[57] D. Samanta, B. Samanta, A.K. Chaudhuri, K. Ghorai, U. Pal, Electrical characterization of stable air-oxidized CdSe films prepared by thermal evaporation. Semicond. Sci. Technol. 11 (1996) 548–553.

[58] A.M. Smith, S.M. Nie, Bright and compact alloyed quantum dots with broadly tunable near-infrared absorption and fluorescence spectra through mercury cation exchange. J. Am. Chem. Soc. 133 (2011) 24–26.

[59] A. Prudnikau, M. Artemyev, M. Molinari, M. Troyon, A. Sukhanova, I. Nabiev, A.V. Baranov, S.A. Cherevkov, A.V. Fedorov, Chemical substitution of Cd ions by Hg in CdSe nanorods and nanodots: spectroscopic and structural examination. Mater. Sci. Eng. B 177 (2012) 744–749.

[60] P. Wu, T. Zhao, S. Wang, X. Hou, Semiconductor quantum dots-based metal ion probes. Nanoscale 6 (2014) 43–64.

[61] E. Lifshitz, Evidence in support of exciton to ligand vibrational coupling in colloidal quantum dots. J. Phys. Chem. Lett. 6 (2015) 4336–4347.

[62] T. Noblet, L. Dreesen, S. Boujday, C. Methivier, B. Busson, A. Tadjeddine, C. Humbert, Semiconductor quantum dots reveal dipolar coupling from exciton to ligand vibration, Comm. Chem. 1 (2018) 76.

[63] F.C.M. Spoor, S. Tomic, A.J. Houtepen, L.D.A. Siebbeles, Broadband cooling spectra of hot electrons and holes in PbSe quantum dots, ACS Nano 11 (2017) 6286–6294.

[64] R. Mrad, S.G. Kruglik, N. Ben Brahim, R. Ben Chaâbane, M. Negrerie, Raman tweezers microspectroscopy of functionalized 4.2-nm diameter CdSe nanocrystals in water reveals changed ligand vibrational modes by a metal cation. J. Phys. Chem. C 123 (2019) 24912–24918.

[65] S.G. Kruglik, J.C. Lambry, J.L. Martin, M.H. Vos, M. Negrerie, Sub-picosecond Raman spectrometer for time-resolved studies of structural dynamics in heme proteins. J. Raman Spectrosc. 42 (2011) 265–275.

[66] M.S. Azzaro, M.C. Babin, S.K. Stauffer, G. Henkelman, S.T. Roberts, Can exciton-delocalizing ligands facilitate hot hole transfer from semiconductor nanocrystals? J. Phys. Chem. C 120 (2016) 28224–28234.

[67] J.D. Leger, M.R. Friedfeld, R.A. Beck, J.D. Gaynor, A. Petrone, X. Li, B.M. Cossairt, M. Khalil, Carboxylate anchors act as exciton reporters in 1.3 nm indium phosphide nanoclusters, J. Phys. Chem. Letters 10 (2019) 1833–1839.

[68] Y. Jiang, B. Tian, Inorganic semiconductor biointerfaces, Nat. Rev. Mater. 3 (2018) 473–490.

Graphical Abstract :

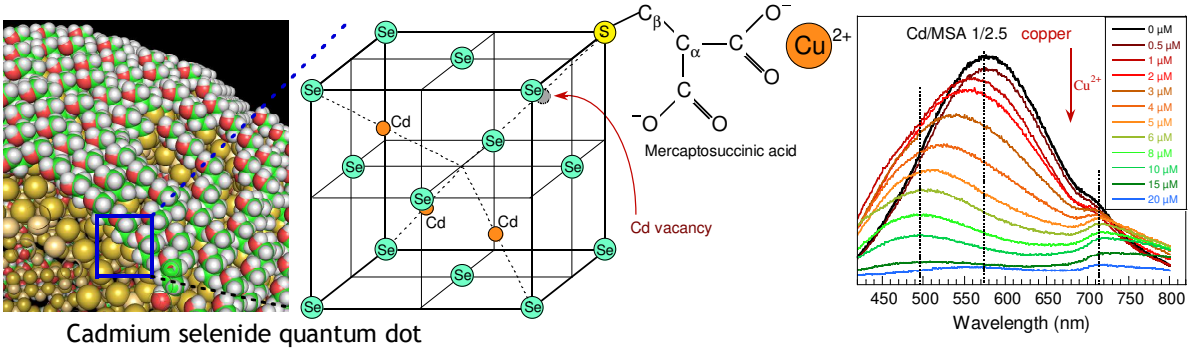

Cadmium selenide quantum dot